buildings

MDPI

Article

Exploring the Effect of Aspect Ratio (H/W) on Thermal Environment in Multiple Climate Zones with Open-Source Data

Jifa Rao [1], Bohong Zheng [1] and Jiayu Li [1,2,3,*]

[1] School of Architecture and Art, Central South University, Changsha 410083, China; raojifa@csu.edu.cn (J.R.); 221312024@csu.edu.cn (B.Z.)
[2] College of Architecture and Urban Planning, Tongji University, Shanghai 200092, China
[3] Hunan Provincial Key Laboratory of Low Carbon Healthy Building, Changsha 410083, China
* Correspondence: jiayuli@alumni.tongji.edu.cn

Abstract: For a country with multiple climate zones, analyzing the impacts of urban design in different climate zones is a prerequisite to climate adaptation policies. However, countries advanced in climate adaptation strategies are mostly located in a single climate zone, leading to a lack of research on climate adaptation policies for multiple climate countries. As China is launching the urban zoning management policy, this research takes China as an example to explore a technique to quickly distinguish the impact of urban design in multiple climate zones by combing the open-source data with the Envi-met tool, where the open-source data indicate the data that can be obtained from public platforms such as the internet and Envi-met is a microclimate simulation tool. First, the open street map tool, one of the open-source data, was used to abstract the typical models of each climate city. Then, open-source meteorological data were employed as the boundary conditions for Envi-met simulation. Lastly, after the Envi-met simulation, the impacts of aspect ratio (H/W) on multiple climate indicators in seven climate cities were analyzed with the meteorological interpolation method. The analytical results show that H/W has a stronger ability to regulate the thermal comfort of high latitude cities. In Guangzhou and Changsha, the maximum differences of PET caused by H/W are only 0.61 °C (Changsha) and 0.63 °C (Guangzhou). H/W has the strongest regulating effect on the thermal comfort in Harbin, with the highest value of 8.62 °C. The regulating effects of H/W on outdoor PET in other 4 cities are 4.37 °C in Urumqi, 3.29 °C in Xining, 1.29 °C in Xi'an, and 0.76 °C in Kunming. In addition, H/W mainly affects PET by modifying the radiant temperature. Compared with mean radiant temperature, the effects of H/W on air temperature, relative humidity, and wind speed are negligible. Longitude regulates the occurrence time of the coldest and hottest thermal environments. Among the seven climate zones in China, the difference in appearance time between the coldest and hottest reaches up to 2 h. For the implementation of urban zoning management policy, in China, high latitude cities are encouraged to high H/W to create a comfortable city. Cities whose latitude is less than 30° may not consider the impacts of H/W on thermal comfort. This method of combining open-source data with Envi-met can serve as a reference for other countries that span multiple climate zones. In addition, these results provide a decision-making basis for the management of H/W in different climate cities of China.

Keywords: thermal comfort; aspect ratio; Envi-met; multiple climate zones

Citation: Rao, J.; Zheng, B.; Li, J. Exploring the Effect of Aspect Ratio (H/W) on Thermal Environment in Multiple Climate Zones with Open-Source Data. *Buildings* **2024**, *14*, 342. https://doi.org/10.3390/buildings14020342

Academic Editors: Wanlu Ouyang, Sheng Liu and Tobi Eniolu Morakinyo

Received: 27 November 2023
Revised: 10 January 2024
Accepted: 18 January 2024
Published: 26 January 2024

1. Introduction

Over the past few decades, rapid urbanization has resulted in higher thermal loads, significantly affecting the energy demand and the health of the residents [1–3]. Many countries have taken actions to mitigate the urban heat island, for example, the garden city of Singapore and "Guideline for the planning, Execution and Upkeep of Green-Roof Sites" of Germany [4,5]. However, most of these countries that are advanced in climate adaption only have one climate zone where climate adaptation policies are easy to formulate.

However, this issue in countries that span multiple climate zones is more complex. For example, China have also promoted greening and controlled the urban morphology though incentive or mandatory policies in the last decades [6]. But the achievements of these actions are not satisfactory as China has many climate zones, where the mandatory policy that is performing well in one climate zones may not be effective in another climate zone [7]. This is easy to understand as thermal perception is formed by regional climate and built environment. For example, a study pointed out that H/W being 1.0 can provide a "cold island area" for cities in arid regions [8], while another study in a hot and humid zone indicated that H/W exceeding 2.0 effectively prolonged daytime shade [9]. Research conducted in a Mediterranean city showed that H/W increased to 3.0 could effectively reduce PET effectively by 4.0 °C [10]. Whether the H/W is 1.0, 2.0, or 3.0, the conclusions are all correct in their respective regions, but may be incorrect in other climate cities. In addition, all these conclusions are driven from three methods, field measurement, wind tunnel experiment, and numerical simulation, which are widely used to explore the impacts of urban morphology on the thermal environment [11,12]. However, for the multiple climate cities, both field measurement and the wind tunnel experiments bring enormous time and economic costs [13]. Although numerical simulation is acceptable, in the view of time and economic costs, extensive work of data collection and simulation often brings difficulties to research. Therefore, it is of significance to explore a method to quickly identify the appropriate space for different climatic zones, which is urgent for countries like China that is launching its urban management policies based on climate zones [14].

To explore a technical path to adaptive to multiple cities research, this research combines the open-source data with the Envi-met tool to simplify the research workload. In this research, open-source data include open street map data and open-source meteorological data [15]. Open street map is non-profit data, which is built by public feedback. Open street map provides urban road and building data globally. With the help of open street map, this research will obtain the urban map easily. In addition, open-source meteorological data are easy to understand, as many countries have published meteorological statistics on their websites. The website of open-source meteorological data in this research are detailed introduced in the next chapter.

Based on the open-source data, this study proposes a technical path to simplify the research workload towards multiple climate zone and clarifies how H/W impacts thermal comfort in multiple climate zones in China. The method proposed in this manuscript can be used in many countries as a more time-saving and cost-effective method.

2. Materials and Methods

2.1. Research Methodological Framework

The research consisted of 8 steps. Step 1, seven typical cities were selected to analyze the impact of H/W on the thermal environment. Step 2, meteorological parameters of those seven cities were collected. Step 3, with the help of Landsat 8, satellite images of the seven cities were obtained which were converted to identify the UHI of each city. Step 4, the texture of typical heat island in each city was extracted by the open street map tool, which provides the UHI area with the information of building and road. Step 5, the H/W of UHI area were calculated from the satellite images with the tool of ArcGIS. Step 6, the typical street models of seven cities were built according to the texture from Step 4 and the H/W from Step 5. Step 7, after the accuracy of the Envi-met tool was validated, the thermal environments were simulated with the variation of H/W in different climate cities. Step 8, the outputs of the research were analyzed. Figure 1 describes the research design of the study. The 8 steps are described in detail in Sections 2.2 and 2.3.

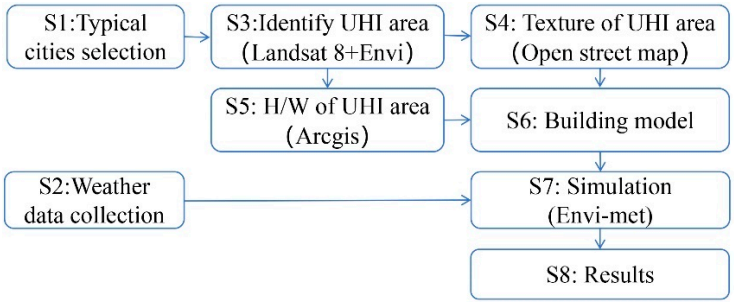

Figure 1. Research design.

2.2. Seven Building Climate Zones in China

2.2.1. Building Climate Zones and Climate Cities

China has 7 building climate zones, shown in Table 1, which are severe cold zone (I), severe cold zone (II), cold zone (I), cold zone (II), warm zone, hot summer–cold winter zone, and hot summer–warm winter zone [16,17]. Based on the following three criteria, 7 typical cities in 7 climate zones were selected. Firstly, the seven cities were the provincial capitals in each climate zone, with high levels of economic development, urbanization, and population density. Secondly, the seven cities are evenly distributed across the climatic zones, with latitudinal positions spanning more than 20 degrees. Thirdly, as highly urbanized central cities, urban heat islands and thermal environment issues were equally prominent in these cities. Harbin (45.63° N, 127.97° E), Xi'an (34.26° N, 108.93° E), Changsha (28.15° N, 113.23° E), Guangzhou (23.27° N, 113.51° E), Kunming (25.29° N, 102.82° E), Xining (36.82°N, 101.44° E), and Urumqi (43.42° N, 87.32° E) were selected as a result.

Table 1. Seven building climate zones in China.

Building Climate Zones	Climate Indicators	Climate Cities
Severe cold zone (I)	January mean $T_a \leq -10$ °C, July mean $T_a \leq 25$ °C July mean RH$\geq$ 50%	Harbin
Severe cold zone (II)	-20 °C $\leq$ January mean $T_a \leq -5$ °C July mean $T_a \geq 18$ °C, July mean RH $\leq$ 50%	Urumqi
Cold zone (I)	-10 °C $\leq$ January mean $T_a \leq 0$ °C 18 °C $\leq$ July mean $T_a \leq 28$ °C	Xi'an
Cold zone (II)	-22 °C $\leq$ January mean $T_a \leq 0$ °C July mean $T_a \leq 18$ °C	Xining
Warm zone	0 °C $\leq$ January mean $T_a \leq 13$ °C 18 °C $\leq$ July mean $T_a \leq 25$ °C	Kunming
Hot summer–cold winter zone	0 °C $\leq$ January mean $T_a \leq 10$ °C 25 °C $\leq$ July mean $T_a \leq 30$ °C	Changsha
Hot summer–warm winter zone	January mean $T_a \geq 10$ °C 25 °C $\leq$ July mean $T_a \leq 29$ °C	Guangzhou

2.2.2. Meteorological Data of Seven Cities

By visiting the open meteorological websites (https://www.cma.gov.cn/, https://xihe-energy.com/), a statistical website for official meteorological data in China, this research collected the meteorological data of the hottest month in seven cities and plotted Figures 2–5. The data shown in Figures 2–5 were used as the boundary condition in the following simulations.

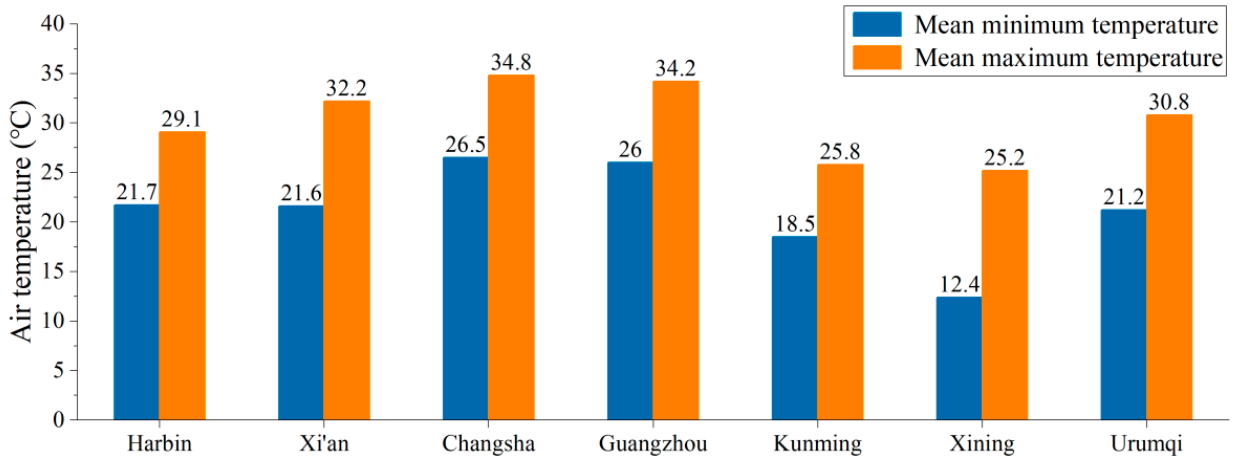

Figure 2. Air temperature data of seven cities.

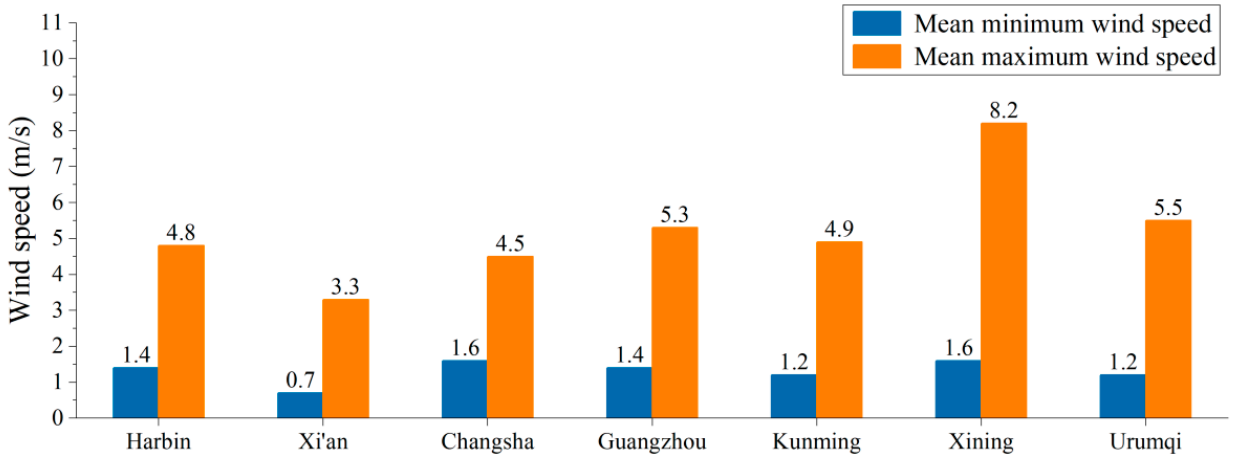

Figure 3. Wind speed data of seven cities.

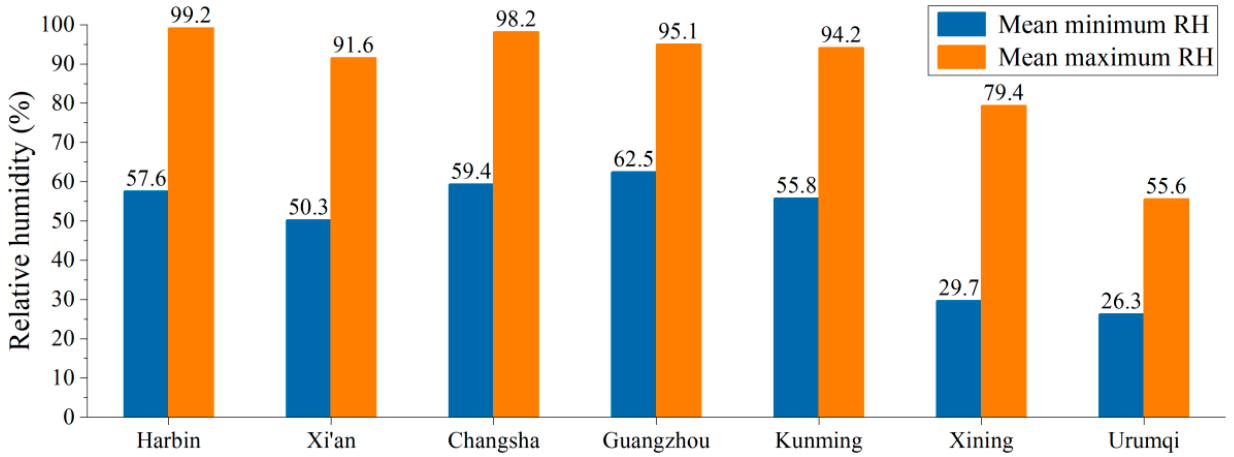

Figure 4. Relative humidity data of seven cities.

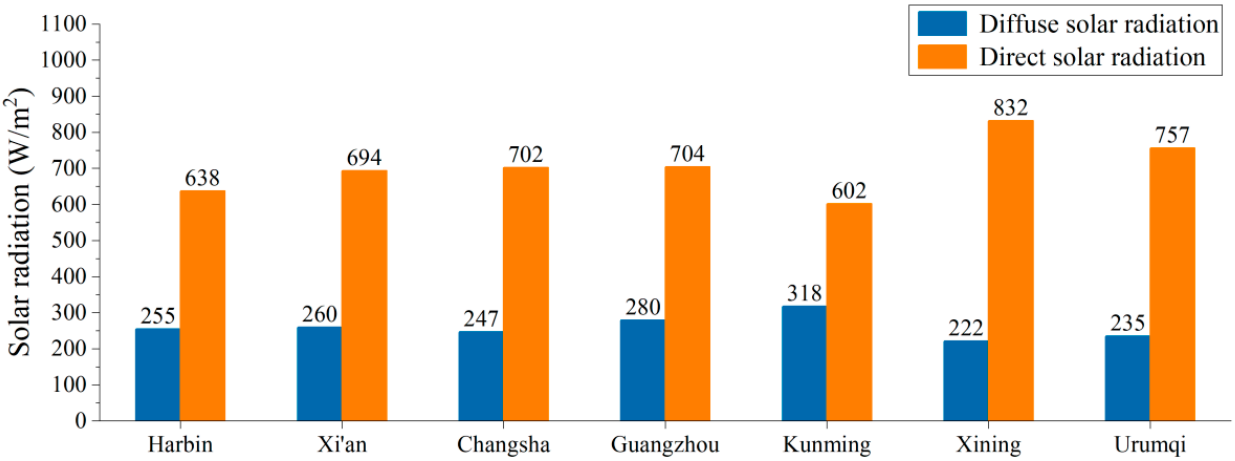

Figure 5. Solar radiation data of seven cities.

2.2.3. Analysis of Building Forms within Heat Island Areas of Seven Cities

The seven building climate zones in China have different climates, cultures, and histories, which contribute to their diversity in urban morphology [18]. This research used "Landsat 8 + open street map" to analyze the spatial form within the strongest urban heat island. Firstly, the study acquired summer remote sensing images from https://www.gscloud.cn, the official data platform of China Institute of Geography. These remote sensing images were inverted to the land surface temperature (LST) in the Arcgis platform, the most powerful geographic information technology that can translate land surface temperature and calculate street height to weight. The method used to calculate LST is shown in Equations (1) and (2) [19]:

$$L_{sen} = B(T_{sen}) = (\varepsilon B(T_s) + (1-\varepsilon)L_d)\tau + L_u \quad (1)$$

$$T_s = \frac{K_2}{\ln\left(\left(\frac{K_1}{B(T_s)}\right)+1\right)} \quad (2)$$

where L_{sen} is the radiance measured by the sensor ($W{\cdot}m^{-2}{\cdot}sr^{-1}{\cdot}\mu m^{-1}$), B is Planck's law, T_{sen} is the radiance brightness measured by the sensor (K), ε is the land surface emissivity, τ is the atmospheric transmissivity, T_s is the land surface temperature (K), L_d is the downwelling atmospheric radiance, L_u is the upwelling atmospheric radiance ($W{\cdot}m^{-2}{\cdot}sr^{-1}{\cdot}\mu m^{-1}$), and K_1 and K_2 are the radiation constants.

The urban heat islands calculated from Landsat 8 are shown in Figure 6, where the most severe heat island of each city was chosen from the urban heat islands. Then, with the tool of open street map, the most comprehensive open-source data platform that provides global street data, we converted the three-dimensional spatial model of each severe heat island, which is shown as the building layout in Figure 6. Based on the classification criteria of spatial morphology [20], we extracted spatial prototypes of different urban heat islands, shown as a typical street model in Figure 7.

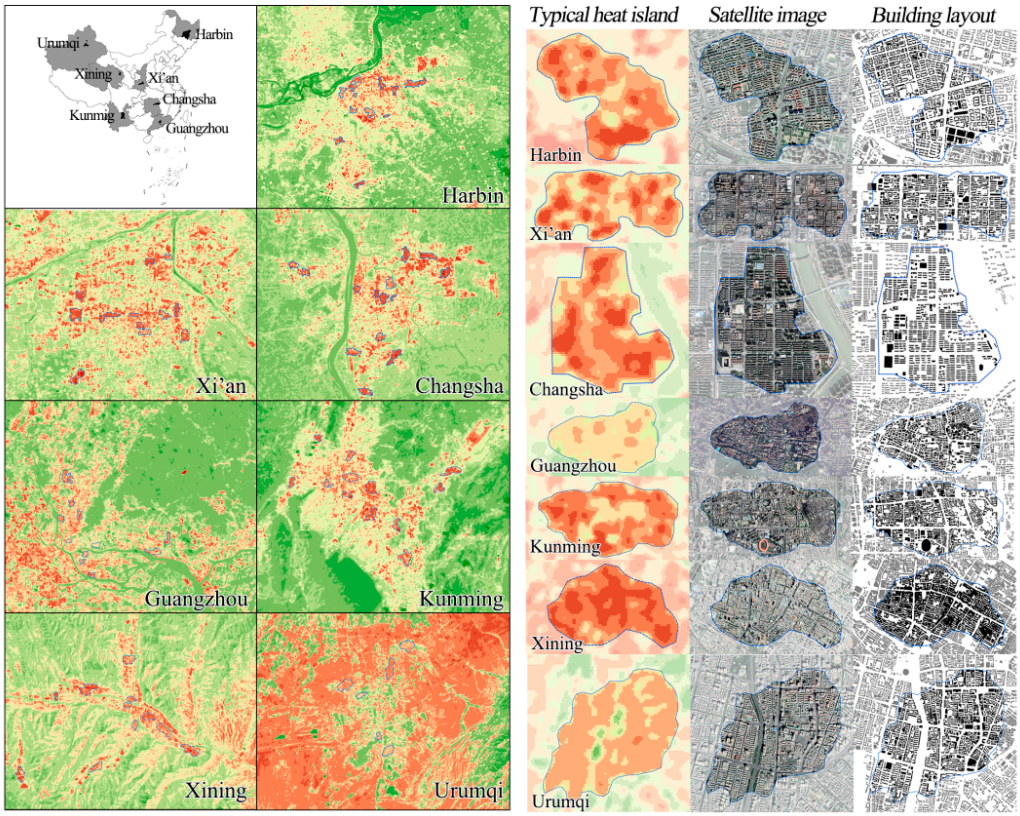

Figure 6. Typical heat island areas and building forms in seven cities.

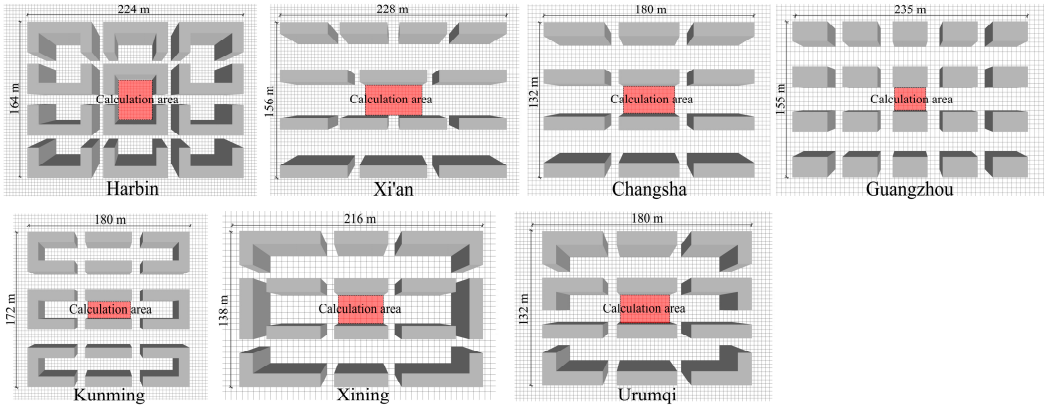

Figure 7. Typical street model of seven cities.

In Figure 7, a calculated area surrounded by the buildings is defined in each subgraph, which is marked in red. In this research, we calculated the average meteorological indicators within the area highlighted in red, as it reflects the general impacts of urban morphology on the outdoor thermal environment.

2.3. Modeling for Climate Cities

With the tool ArcGIS, which can calculate the height of buildings based on the shadows of remote sensing data, this research calculated the H/W of the streets entitled as the building layout in Figure 8 [21]. The analytical results indicated that the H/W of high latitude cities was slightly higher than that of low latitude cities. In general, the H/W in Guangzhou, Changsha, and Kunming were observed in the range of 1 to 2.5, and the lowest SVFs in Harbin and Urumqi were 0.5. For comparability, this research took 0.5, 1.0, 1.5, 2.0, and 2.5 as the cases to build models, shown in Figure 8. In Figure 8,

due to the diversity of building layout, the building densities were different, which were 23.7 (Harbin), 22.2% (Xi'an), 23.5% (Changsha), 24.1%(Guangzhou), 25.3% (Kunming), 24.2% (Xining), and 25.4% (Urumqi). In Figure 8, subgraphs a, b, c, d, and e are correspond to the model with the H/W of 0.5, 1.0, 1.5, 2.0, and 2.5.

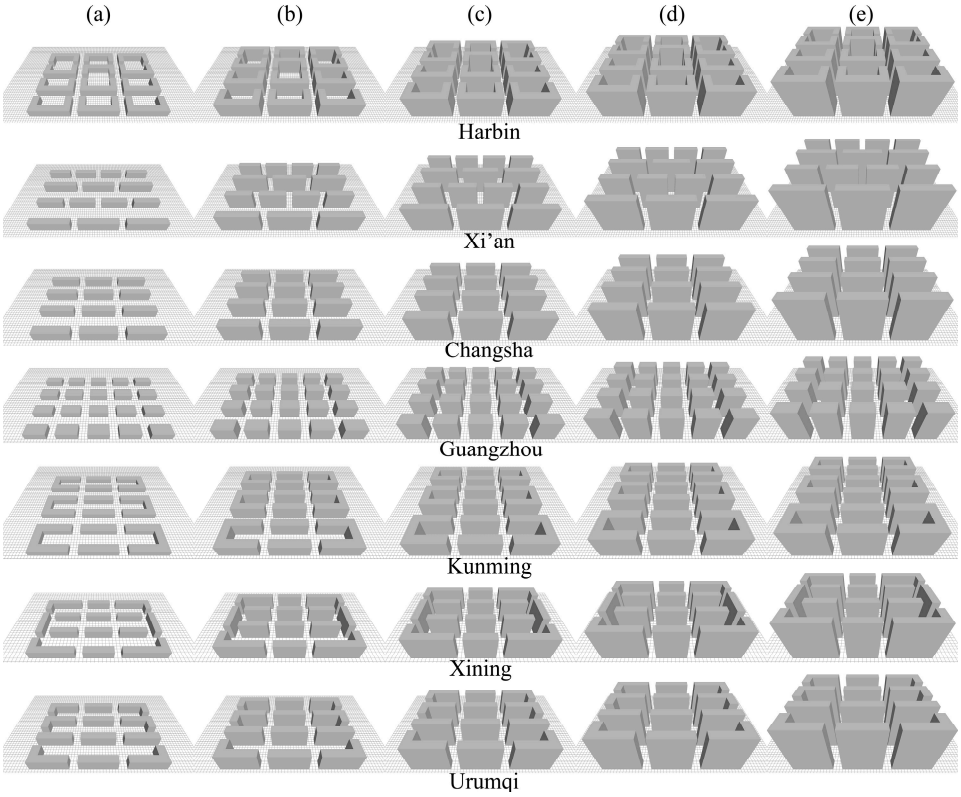

Figure 8. (**a**–**e**) Envi-met model with five H/W values for seven cities. **Harbin**: building density being 23.7%; **Xi'an**: building density being 22.2%; **Changsha**: building density being 23.5%; **Guangzhou**: building density being 24.1%; **Kunming**: building density being 25.3%; **Xining**: building density being 24.2%; **Urumqi**: building density being 25.4%.

2.4. Validation of the Envi-met

Envi-met is an advanced microclimate simulation tool that has been widely used by urban planners. To confirm the accuracy of the Envi-met model, we conducted a measurement experiment, which was carried out in Changsha, shown in Figure A1 of the Appendix A. In this experiment, the micro-weather station was used, whose accuracy is detailed in Table A1 of the Appendix A. The measurement lasted for 12 months, where 4 typical days in January (winter), April (spring), July (summer), and October (winter) were selected to analyze. The measured and simulated data collected from the 4 typical days are shown in Figure A2 of the Appendix A. The coefficient of determination (R^2) [22], root mean square error (RMSE) [23], and mean absolute error (MAE) were analyzed between the simulated and measured data [24], whose equations are shown as Equations (3)–(5). In the equations, $X_{m;\,i}$ represents the measured value, and $X_{s;\,i}$ represents the simulated value; n represents the number of data.

$$R^2 = 1 - \frac{\sum_{i=1}^{n}\left(X_{m;\,i} - X_{s;\,i}\right)^2}{\sum_{i=1}^{n}\left(X_{m;\,i} - \overline{X}\right)^2} \tag{3}$$

$$RMSE = \sqrt{\frac{\sum_{i=1}^{n}\left(X_{m;\,i} - X_{s;\,i}\right)^2}{n}} \tag{4}$$

$$MAE = n^{-1}\sum_{i=1}^{n}|X_{m;\,i} - X_{s;\,i}| \quad (5)$$

The analytical results indicated that the R^2, RMSE, and MAE of air temperature were 0.99 °C, 1.76 °C, and 0.68 °C. The R^2, RMSE, and MAE of relative humidity were 0.98%, 3.61%, and 1.50%, respectively. Compared with previous studies, the R^2 of air temperature and relative humidity in this experiment were higher than 0.82 [25], which means excellent fitness. The RMSE and the MAE of the air temperature in this experiment were consistent with Hayder Alsaad's validation results [26]. The RMSE and MAE of relative humidity were below 8.77% and 7.78% [27], a threshold standard believed in previous research. The validated experiment proved that Envi-met is reliable in simulating the thermal environment.

3. Results

The meteorological data in the results section all refer to the average of the calculation area. For example, the air temperature at 8:00 in Harbin was 24.5 °C (H/W = 0.5), which means that the average air temperature of the calculated aera was 24.5 °C. To visually display the effects of H/W on the daily thermal environment, this research used the temperature interpolation method [28], which is shown as Figures 9–13. In these figures, each point has three attributes (X, Y, Z), namely the horizontal axis X, vertical axis Y, and Z values. X represents the time on that day, Y represents the H/W value, and Z represents the meteorological data value under this scenario.

3.1. Effect of Aspect Ratio on Air Temperature

Based on the principle of the thermal distribution map, this research drew the air temperature maps that affected by the H/W in seven cities of the severe hot day, which are shown in Figure 9.

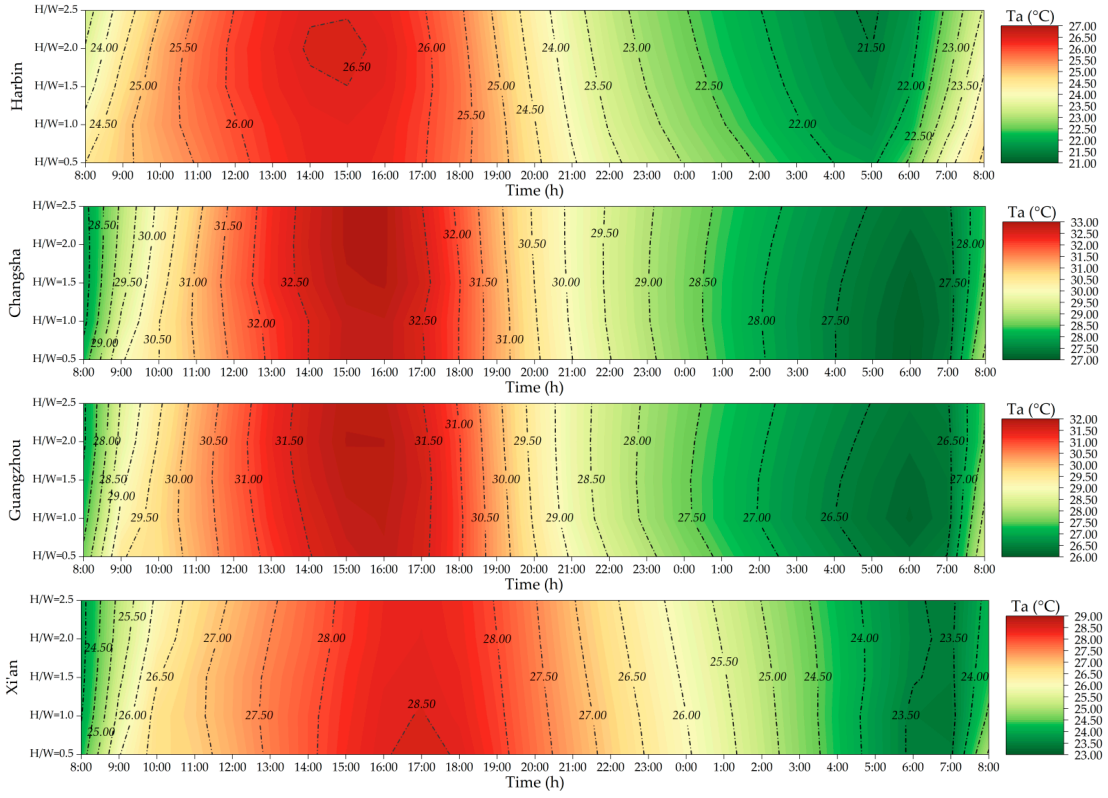

Figure 9. *Cont.*

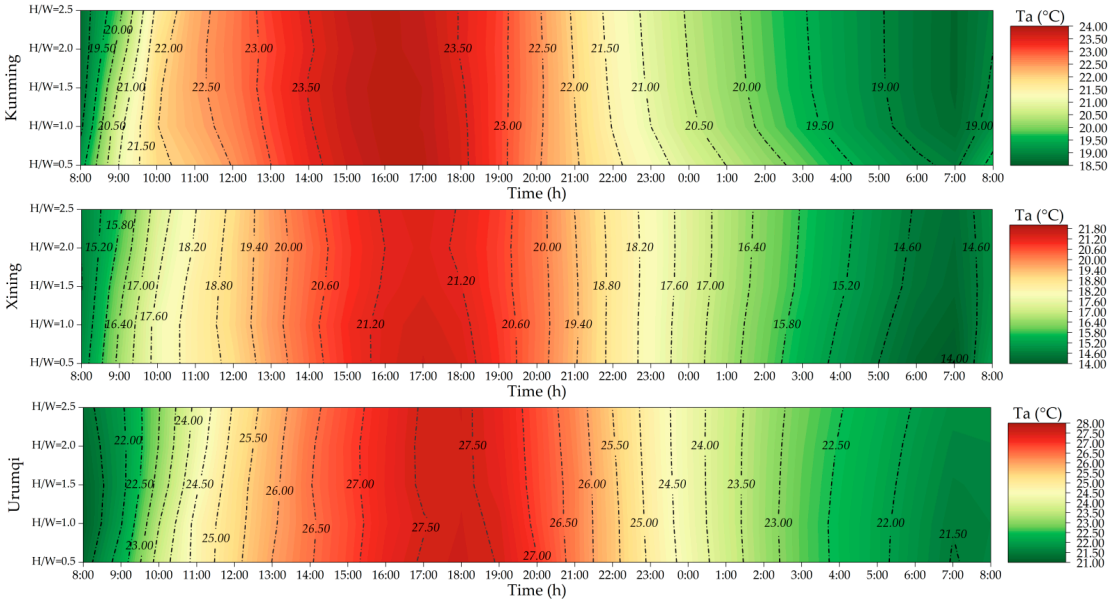

Figure 9. Hourly distribution of air temperature in seven cities.

From Figure 9, it can be seen that the hottest air temperature of Harbin happened around 15:00, and that of Changsha and Guangzhou happened around 16:00. For Xi'an, Kunming, Xining, and Urumqi, the hottest air temperatures were delayed until around 17:00. This is caused by the difference in longitude among the seven cities. With the higher longitude, the later the hottest time period appears. Similarly, the occurrence time of the lowest temperature at night was consistent with that of the highest temperature during the day. For Harbin, the lowest air temperature of the day occurred at 5:00, and that of Changsha and Guangzhou occurred at 6:00. The lowest air temperatures of Xi'an, Kunming, Xining, and Urumqi occurred around 7:00.

For Harbin, Changsha, and Guangzhou, high H/W improved the outdoor air temperatures since the highest air temperature of these streets occurred when H/W was around 2.0 to 2.5. Meanwhile, high H/W decreased the outdoor air temperatures in Xi'an and Xining. Kunming and Urumqi were not sensitive to H/W in terms of outdoor air temperature.

To quantitively analyze the impacts of H/W on outdoor air temperatures in different climate cities, this research analyzed the maximum air temperatures of each city under the five H/W scenarios, shown in Table 2. The analytical results in Table 2 confirm that Kunming and Urumqi are not sensitive to H/W in terms of outdoor air temperature.

Table 2. Maximum air temperature in seven cities.

City	H/W					Range
	0.5	1.0	1.5	2.0	2.5	
Harbin	26.38 °C	26.42 °C	26.50 °C	26.56 °C	26.48 °C	0.18 °C
Xi'an	28.58 °C	28.51 °C	28.47 °C	28.42 °C	28.41 °C	0.17 °C
Changsha	32.81 °C	32.82 °C	32.93 °C	32.94 °C	32.95 °C	0.14 °C
Guangzhou	31.82 °C	31.85 °C	31.89 °C	31.92 °C	31.90 °C	0.10 °C
Kunming	23.86 °C	23.88 °C	23.90 °C	23.86 °C	23.85 °C	0.05 °C
Xining	21.51 °C	21.48 °C	21.38 °C	21.33 °C	21.36 °C	0.18 °C
Urumqi	27.61 °C	27.59 °C	27.57 °C	27.58 °C	27.59 °C	0.04 °C

3.2. *Effect of Aspect Ratio on Relative Humidity*

Based on the principle of the thermal distribution map, this research drew the relative humidity maps that affected by the H/W in seven cities of the serious hot day, which are shown in Figure 10.

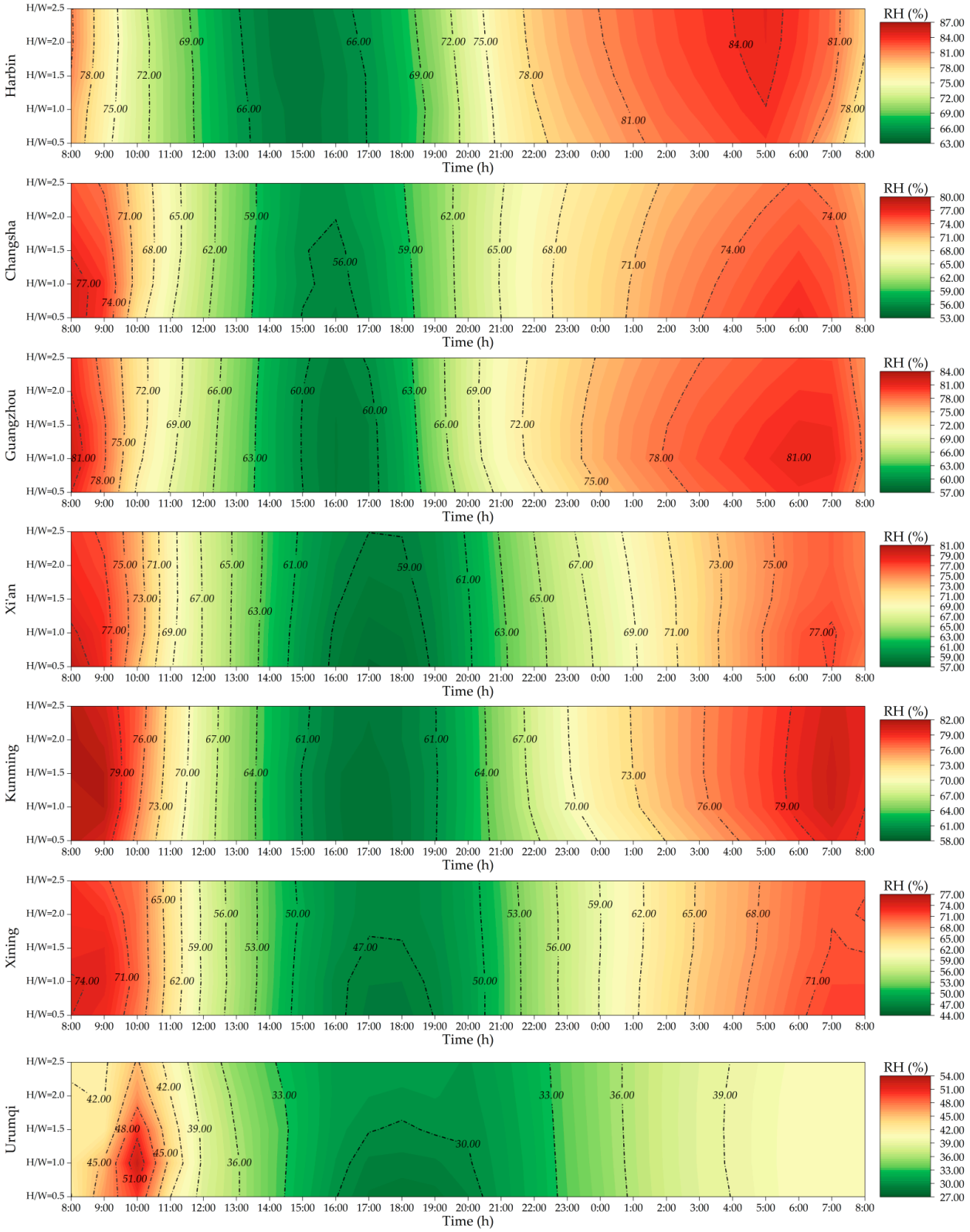

Figure 10. Hourly distribution of relative humidity in seven cities.

From Figure 10, it can be seen that the lowest relative humidity of Harbin happened around 15:00, and that of Changsha and Guangzhou happened around 16:00. For Xi'an, Kunming, Xining, and Urumqi, the lowest relative humidity was delayed until 17:00 and 18:00. The trends of lowest relative humidity ere conversely similar to that of air temperature, because high air temperature will decrease the relative humidity. For the highest relative humidity, their occurrence times were 5:00 (Harbin), 6:00 (Guangzhou and Changsha), 7:00 (Xi'an and Kunming), 8:00 (Xining), and 10:00 (Urumqi).

Except for Harbin, the relative humidity of the other six cities increased with the rise of H/W in daytime, and the relative humidity of the six cities generally decreased with the increase of H/W at night time.

To quantify the impacts of H/W on outdoor relative humidity in different climate cities, this research analyzed the maximum relative humidity of each city under the five H/W scenarios, shown in Table 3. The analytical results in Table 3 indicate that with the increase of H/W, the relative humidity increases at night in the cities except Harbin. In addition, Table 3 also indicates that Xining and Urumqi have the lowest relative humidity, but they are most sensitive to H/W in terms of relative humidity.

Table 3. Minimum relative humidity in seven cities.

City	H/W					Range
	0.5	1.0	1.5	2.0	2.5	
Harbin	64.79%	64.78%	64.65%	64.66%	64.74%	0.14%
Xi'an	57.94%	58.20%	58.48%	58.76%	59.01%	1.07%
Changsha	55.43%	55.64%	55.74%	56.02%	56.26%	0.83%
Guangzhou	58.99%	58.96%	58.98%	59.07%	59.32%	0.36%
Kunming	59.11%	59.15%	59.16%	59.42%	59.56%	0.45%
Xining	46.21%	46.50%	46.91%	47.17%	47.23%	1.02%
Urumqi	28.57%	29.33%	29.86%	30.27%	30.42%	1.85%

3.3. Effect of Aspect Ratio on Wind Speed

The wind distribution maps are shown in Figure 11. Figure 11 indicates that, in general, the wind speed during the day was greater than that during the night in all the seven cities. In addition, for Harbin and Changsha, H/W being 1.0 produced the lowest wind speeds. For Guangzhou, Xining and Urumqi, H/W being 1.5 to 2.0 produced the lowest wind speed. For Kunming and Xi'an, the lowest wind speed occurred when the H/W was 2.5.

In general, the effect of H/W on wind speed was slight. The differences of wind speed in the five H/W cases were 0.13 m/s (Harbin), 0.03 m/s (Xi'an), 0.04 m/s (Changsha), 0.05 m/s (Guangzhou), 0.03 m/s (Xining), and 0.04 m/s (Urumqi), respectively. These differences are shown in Table 4.

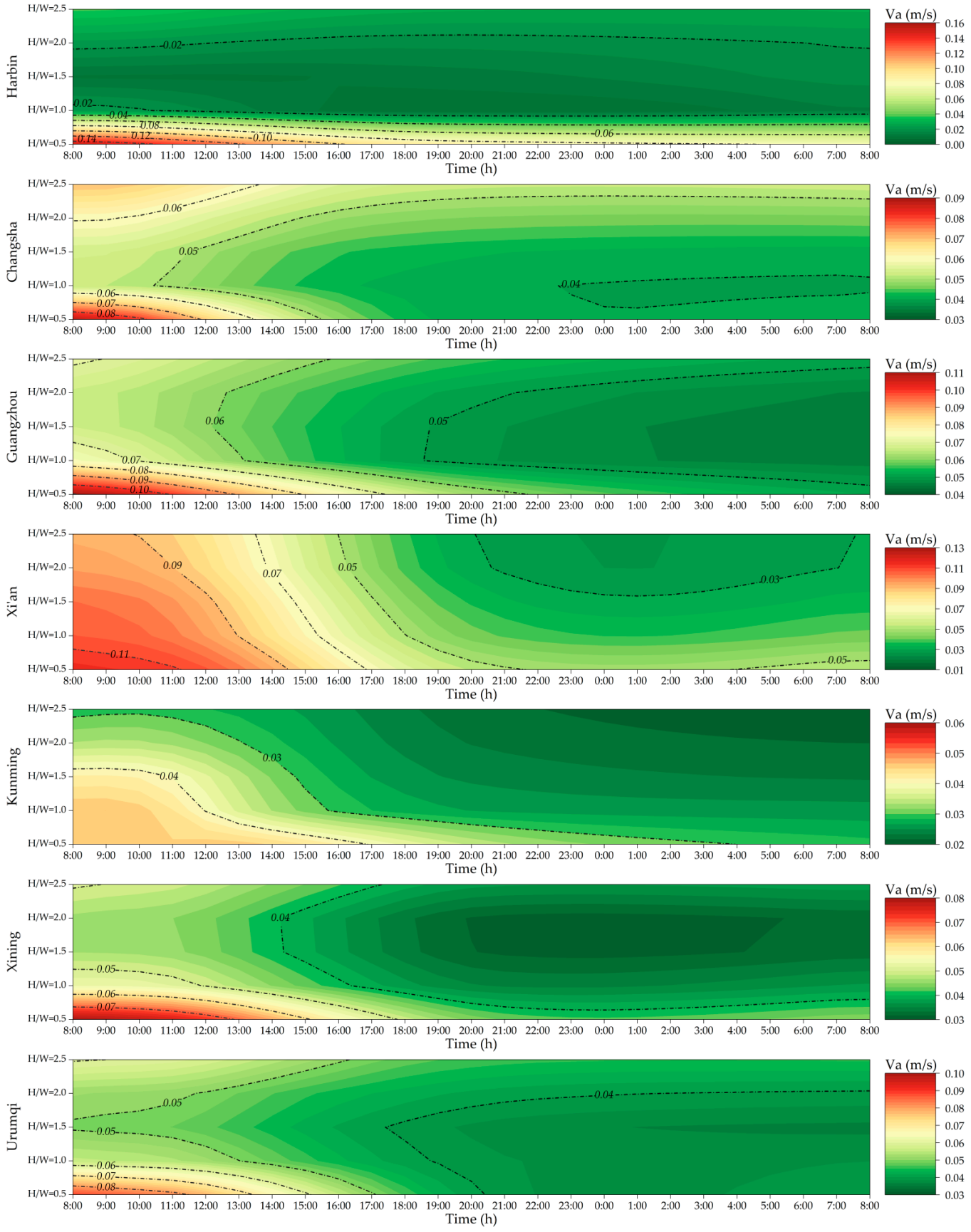

Figure 11. Hourly distribution of wind speed in seven cities.

Table 4. Maximum wind speed in seven cities.

City	H/W					Range
	0.5	1.0	1.5	2.0	2.5	
Harbin	0.15 m/s	0.02 m/s	0.01 m/s	0.02 m/s	0.04 m/s	0.13 m/s
Xi'an	0.12 m/s	0.10 m/s	0.10 m/s	0.09 m/s	0.09 m/s	0.03 m/s
Changsha	0.09 m/s	0.05 m/s	0.05 m/s	0.06 m/s	0.07 m/s	0.04 m/s
Guangzhou	0.11 m/s	0.07 m/s	0.07 m/s	0.06 m/s	0.07 m/s	0.05 m/s
Kunming	0.05 m/s	0.05 m/s	0.04 m/s	0.03 m/s	0.03 m/s	0.02 m/s
Xining	0.08 m/s	0.05 m/s	0.05 m/s	0.05 m/s	0.05 m/s	0.03 m/s
Urumqi	0.09 m/s	0.06 m/s	0.05 m/s	0.05 m/s	0.06 m/s	0.04 m/s

3.4. Effect of Aspect Ratio on Mean Radiant Temperature

The mean radiant temperatures in different H/W scenarios of the seven cities are shown in Figure 12. From Figure 12, it is obvious that the highest mean radiant temperature occurred at different time in the seven cities. In Harbin, the highest mean radiant temperature occurred at 13:00. For Changsha and Guangzhou, the highest mean radiant temperature happened at 15:00. In Xi'an and Kunming, the highest mean radiant temperature occurred at 16:00. Xining and Urumqi experienced the highest radiant temperatures around 17:00. For the lowest mean radiant temperature, the earlier the highest mean radiation temperature appeared, the earlier the lowest mean radiant temperature appeared.

With the growth of H/W, the mean radiant temperature at pedestrian height gradually decreased in the seven cities. This is because high H/W prevents solar radiation entering the street canyon in the daytime, which decreases the mean radiant temperature. During the night, high H/W blocks the loss of longwave radiation, which increases the mean radiation temperature during night.

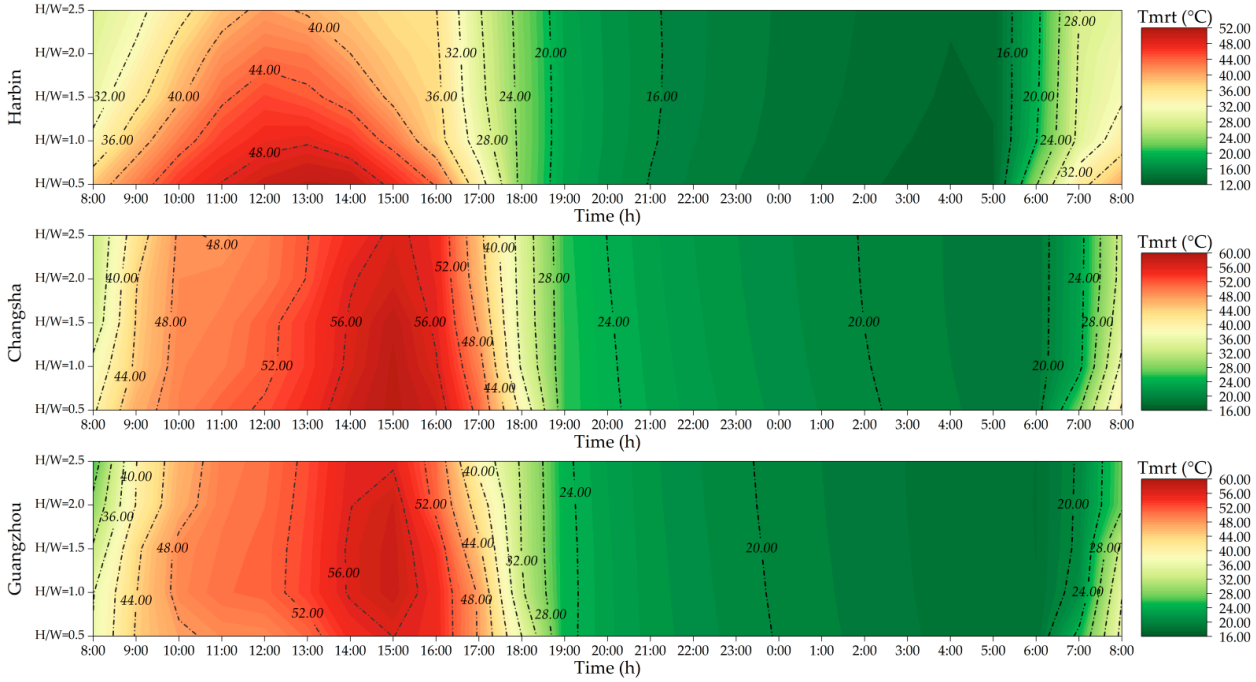

Figure 12. *Cont.*

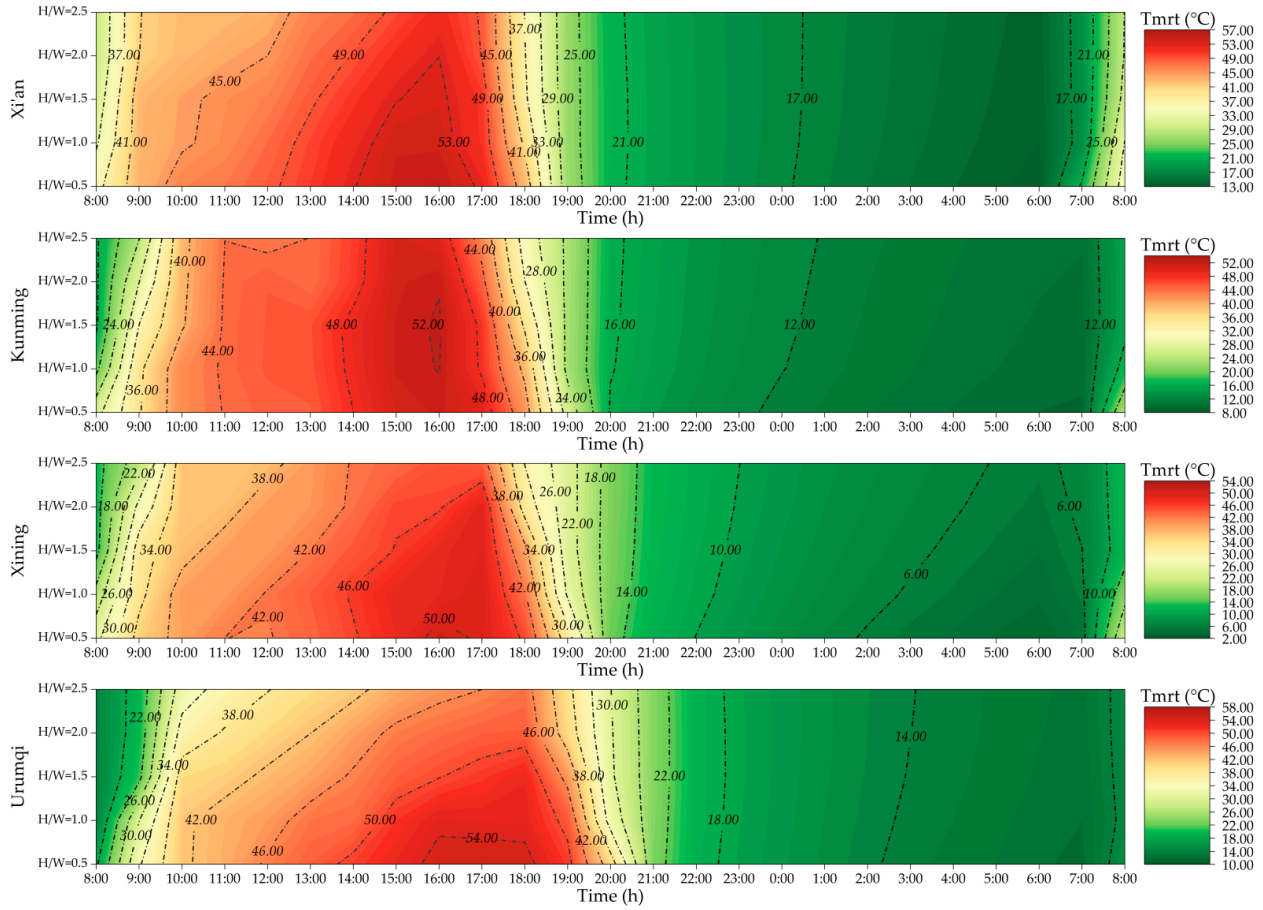

Figure 12. Hourly distribution of Tmrt in seven cities.

To quantify the impacts of H/W on mean radiant temperature in different climate cities, this research analyzed the mean radiant temperature of each city under the five H/W scenarios, shown in Table 5. Table 5 reveals that Harbin, Urumqi, and Xining are more sensitive to the change of H/W in terms of mean radiant temperature. The differences of mean radiant temperature in three cities were 10.09 °C (Harbin), 7.57 °C (Urumqi), and 6.39 °C (Xining). Kunming and Guangzhou were the least sensitive cities to H/W regarding mean radiation temperature in the seven cities, whose impacts on mean radiant temperatures were 1.36° C (Kunming) and 2.14 °C (Guangzhou).

Table 5. Maximum Tmrt in seven cities.

City	H/W					Range
	0.5	1.0	1.5	2.0	2.5	
Harbin	50.89 °C	47.73 °C	45.47 °C	43.06 °C	40.80 °C	10.09 °C
Xi'an	55.26 °C	54.22 °C	53.56 °C	52.98 °C	51.52 °C	3.74 °C
Changsha	58.96 °C	58.90 °C	58.52 °C	57.06 °C	56.56 °C	2.40 °C
Guangzhou	56.04 °C	57.77 °C	57.67 °C	57.42 °C	55.63 °C	2.14 °C
Kunming	51.53 °C	52.06 °C	52.20 °C	51.89 °C	50.84 °C	1.36 °C
Xining	51.01 °C	49.93 °C	49.36 °C	49.06 °C	44.62 °C	6.39 °C
Urumqi	54.99 °C	53.50 °C	52.57 °C	48.79 °C	47.42 °C	7.57 °C

3.5. Effect of Aspect Ratio on Physiological Equivalent Temperature

The impacts of H/W on outdoor thermal comfort in the seven cities were analyzed in Figure 13. Figure 13 illustrates that Guangzhou and Changsha suffer from the hottest thermal perception in summer as the highest PET even exceeds 56 °C in the two cities. For Harbin, Guangzhou, and Xi'an, H/W being 1.0 witnessed the highest PET in the street. For Kunming, the highest PET happened when the H/W is 1.5. For Changsha, Xining, and Urumqi, high H/W reduced the highest PET of the day.

For PET, the patterns of change are more diverse since the PET index is formed by the combination of temperature, wind speed, humidity, and other indicators. PET is not a direct physical indicator affected by morphology.

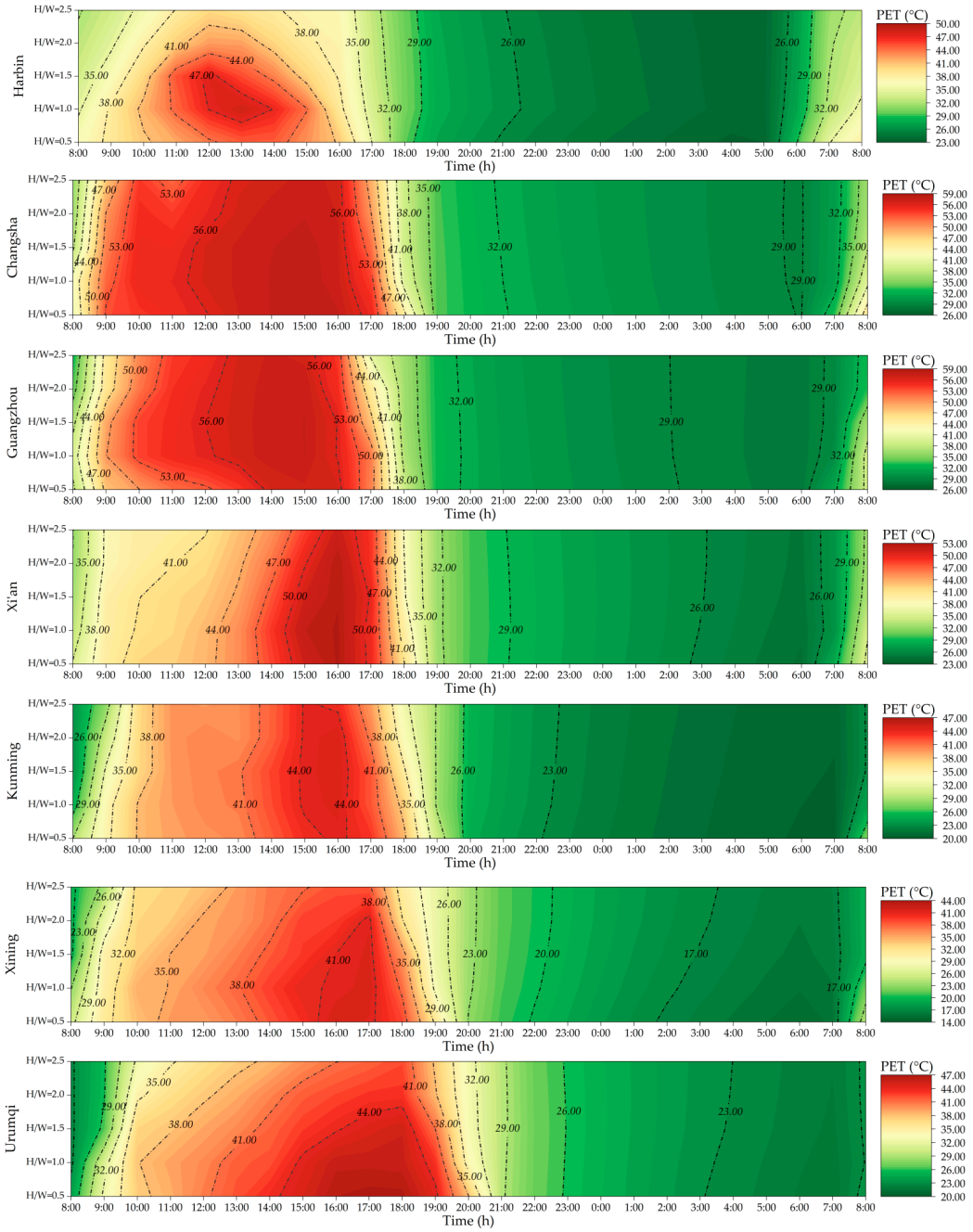

Figure 13. Hourly distribution of PET in seven cities.

To quantify the impacts of H/W on outdoor thermal comfort in different climate cities, this research analyzed the highest PET in seven cities, shown in Table 6. Table 6 illustrates that although Changsha and Guangzhou suffer from the most severe hot PET, H/W had the weakest power in regulating the PET. In Guangzhou and Changsha, the maximum differences of PET caused by H/W were only 0.61 °C (Changsha) and 0.63 °C (Guangzhou). H/W had the strongest regulating effect on the thermal comfort in Harbin, with the highest value of 8.62 °C. The regulating effects of H/W on outdoor PET were 4.37 °C in Urumqi, 3.29 °C in Xining, 1.29 °C in Xi'an, 0.76 °C in Kunming, 0.63 °C in Guangzhou, and 0.61 °C in Changsha.

Table 6. Maximum PET in seven cities.

City	H/W					Range
	0.5	1.0	1.5	2.0	2.5	
Harbin	44.87 °C	48.45 °C	47.54 °C	42.41 °C	39.83 °C	8.62 °C
Xi'an	52.50 °C	52.59 °C	52.44 °C	52.47 °C	51.30 °C	1.29 °C
Changsha	57.74 °C	57.86 °C	57.80 °C	57.44 °C	57.25 °C	0.61 °C
Guangzhou	56.88 °C	57.5 °C	57.51 °C	57.46 °C	57.12 °C	0.63 °C
Kunming	44.30 °C	44.68 °C	44.91 °C	44.87 °C	44.15 °C	0.76 °C
Xining	42.10 °C	41.88 °C	41.61 °C	41.43 °C	38.81 °C	3.29 °C
Urumqi	46.78 °C	45.84 °C	45.44 °C	43.25 °C	42.41 °C	4.37 °C

4. Discussion

Urban morphology, vegetation [29,30], and reflectance [31] are the three main channels to mitigate urban heat island. This research explored the effects of H/W, an urban morphology indicator, on thermal environment. The above results indicate that, compared with mean radiant temperature, the effects of H/W on air temperature, relative humidity, and wind speed are negligible, which is consistent with previous studies [4,32]. Previous studies have clarified that high H/W blocks the access of solar radiation to the street, which significantly affects the mean radiant temperature [33]. In this study, air temperatures sometimes were observed to increase with the rise of H/W in Harbin, Changsha, Guangzhou, and Kunming, which was caused by high H/W storing more heat in buildings. Therefore, it is easy to understand that similar phenomenon is commonly seen at nighttime in these cities. High H/W is also reported to reduce the wind speed by its high wind resistance [34], which was also confirmed in this research, especially in Harbin, whose wind speed reduced from 0.14 m/s to 0.02 m/s with the increase of H/W in this research. Wind speed is not an effective channel for H/W regulating thermal comfort. This is because the impacts of H/W on wind speed in the seven cities are far from the perceptible wind speed. Previous studies have confirmed that high H/W leads to a reduction in mean radiant temperature [35], which is consistent with the results of this study. The increase of H/W could increase the shade covering the street [36], reducing the mean radiant temperature. In this study, with H/W increased to 2.5, the mean radiant temperatures were reduced by 3.74 °C (Xi'an), 6.39 °C (Xining), 7.57 °C (Urumqi), and 10.09 °C (Harbin).

Compared to low latitude cities, the solar incidence angle in high latitude cities decreases, which makes it more sensitive the H/W. This study further analyzed the impacts of H/W on thermal indicators in these cities, confirming that high latitude cities are more sensitive to the H/W in terms of regulating the thermal environment. For instance, the regulating power of H/W on mean radiant temperature in Harbin was several times that of Changsha and Guangzhou.

Although air temperature and relative humidity increased with the rise of H/W in the daytime, their effects were very weak compared to the mean radiant temperature. As the mean radiant temperature decreases with the rise of H/W, hence the PET also decreases

with the increase of H/W in the daytime. So, from the results of this study, we also confirmed that H/W mainly regulates PET by the channel of mean radiant temperature.

For the urban zoning governance policy, Guangzhou and Changsha are not sensitive to the change of H/W. Therefore, climate adaptive cities for Guangzhou and Changsha may not consider the impact of H/W. For Harbin, H/W being 1.0 to 1.5 is not conducive to its thermal comfort in summer. For the other four cities, high H/W is encouraged to build the urban climate adaptive city.

5. Conclusions

This study proposes and exemplifies a method to explore the impact of H/W on the thermal environment across multiple climate zones with open-source data and the Envi-met tool, which reduces the time and economic cost of investigation. This method can be used in any country to research its climate adaptation policies. In addition, this research clarifies the effect of H/W on the thermal environment in multiple climate zones in China and identifies the best H/W for each climate zone, which are helpful for policy-making based on climate zones. The results can be summed up as follows:

- H/W had a stronger ability to regulate the thermal comfort of high latitude cities. In Guangzhou and Changsha, the maximum differences of PET caused by H/W were only 0.61 °C (Changsha) and 0.63 °C (Guangzhou). H/W had the strongest regulating effect on the thermal comfort in Harbin, with the highest value of 8.62 °C. The regulating effects of H/W on outdoor PET in other four cities were 4.37 °C in Urumqi, 3.29 °C in Xining, 1.29 °C in Xi'an, and 0.76 °C in Kunming.
- H/W mainly affects PET by modifying the radiant temperature. Compared with mean radiant temperature, the effects of H/W on air temperature, relative humidity, and wind speed are negligible.
- Longitude regulates the occurrence time of the coldest and hottest environments. Among the seven climate zones in China, the difference in appearance time between the coldest and hottest time of day reached up to 2 h.

Therefore, from the view of a climate adaptive city, high latitude cities are encouraged to high H/W to create a comfortable city. Cities at low latitude are slightly affected by the H/W in terms of thermal comfort. Therefore, cities whose latitude is less than 30°, may not consider the impacts of H/W on thermal comfort.

This study enhances our understanding of the thermal comfort regulated by H/W across multiple climate zones. This study has several limitations which need further exploration. Firstly, Envi-met constructs ideal urban models, and complex urban models should be explored in subsequent studies. Secondly, this study focused on the impact of H/W on thermal environments without considering its impact on air pollutants. Evaluating the H/W from the view of both the thermal environment and air pollutants deserve further study.

Author Contributions: Conceptualization, J.L.; methodology, J.L.; software, J.R.; validation, J.R. and B.Z.; formal analysis, J.R.; investigation, B.Z.; resources, B.Z.; data curation, J.R.; writing—original draft preparation, J.R.; writing—review and editing, J.L.; visualization, J.L.; supervision, B.Z.; project administration, J.L.; funding acquisition, J.L. All authors have read and agreed to the published version of the manuscript.

Funding: This research was funded by Hunan Provincial Natural Science Foundation, grant number 2023JJ40728, 2023JJ30693; the Hunan Provincials Philosophy and Social Science Achievement Evaluation Committee Project, grant number XSP22YBZ094; and the Scientific Research Fund of Hunan Provincial Education Department, grant number 21B0186.

Data Availability Statement: The raw data supporting the conclusions of this article will be made available by the authors on request.

Conflicts of Interest: The authors declare no conflicts of interest.

Appendix A

The micro weather station is shown in Figure A1. The metrics of the weather station instruments are shown in Table A1. The data of the measured and simulated air temperatures and relative humidity are shown in Figure A2.

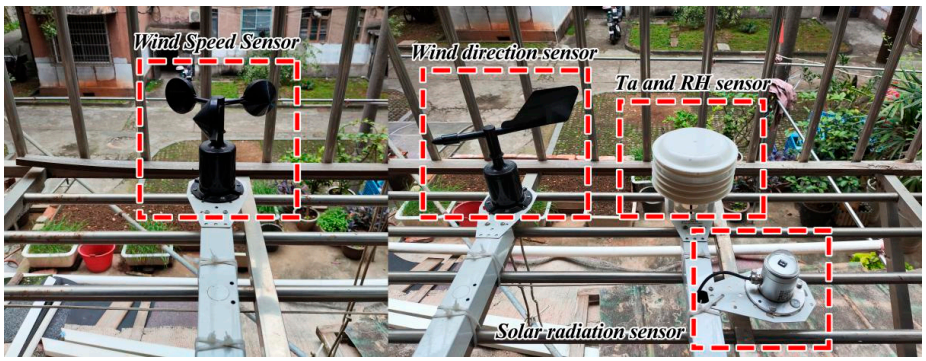

Figure A1. The micro weather station was fixed near the building.

Table A1. Introduction of the micro weather station.

Measuring Instruments	Measurement Indicators	Measurement Range	Instrument Precision	Range of Error
Ta and RH sensor	Air temperature	−20 ~ 100 °C	0.1 °C	±0.5 °C
	Relative humidity	0 ~ 100%	0.1%	±0.5%
Wind direction sensor	Wind direction	0 ~ 360°	1°	±3°
Wind speed sensor	Wind speed	0 ~ 70 m/s	0.1 m/s	±0.5 m/s
Solar radiation sensor	Total solar radiation	0 ~ 2000 W/m^2	1 W/m^2	±5 W/m^2

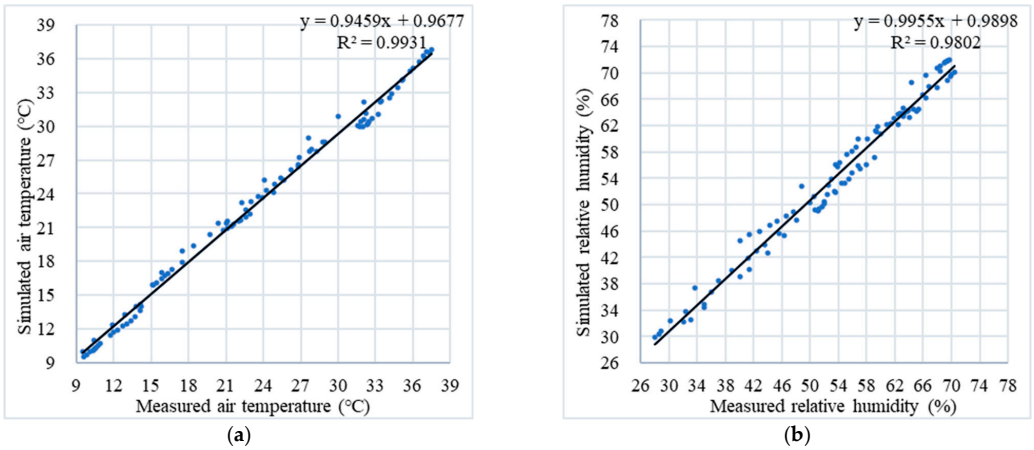

(**a**) (**b**)

Figure A2. (**a**) the distribution of air temperature (simulated and measured data); (**b**) the distribution of the relative humidity (simulated and measured data).

References

1. Tian, L.; Lu, J.; Li, Y.; Bu, D.; Liao, Y.; Wang, J. Temporal characteristics of urban heat island and its response to heat waves and energy consumption in the mountainous Chongqing, China. *Sustain. Cities Soc.* **2021**, *75*, 103260. [CrossRef]
2. Luu, H.T.; Rojas-Arias, J.C.; Laffly, D. The impacts of urban morphology on housing indoor thermal condition in hoi an city, Vietnam. *J. Contemp. Urban Aff.* **2021**, *5*, 183–196. [CrossRef]
3. Mauricio, C.; Palacio, M.; Martínez, A. Experimental analysis of a flat plate solar collector with integrated latent heat thermal storage. *Contemp. Urban Aff.* **2017**, *1*, 7–12.
4. Li, J.; Zheng, B.; Bedra, K.B. Evaluating the improvements of thermal comfort by different natural elements within courtyards in Singapore. *Urban Clim.* **2022**, *45*, 101253. [CrossRef]
5. Dong, J.; Zuo, J.; Luo, J. Development of a management framework for applying green roof policy in urban China: A preliminary study. *Sustainability* **2020**, *12*, 10364. [CrossRef]

6. He, B.-J.; Wang, J.; Zhu, J.; Qi, J. Beating the urban heat: Situation, background, impacts and the way forward in China. *Renew. Sustain. Energy Rev.* **2022**, *161*, 112350. [CrossRef]
7. Li, J.; Zheng, B.; Chen, X.; Qi, Z.; Bedra, K.B.; Zheng, J.; Li, Z.; Liu, L. Study on a full-year improvement of indoor thermal comfort by different vertical greening patterns. *J. Build. Eng.* **2021**, *35*, 101969. [CrossRef]
8. Pearlmutter, D.; Bitan, A.; Berliner, P. Microclimatic analysis of "compact" urban canyons in an arid zone. *Atmos. Environ.* **1999**, *33*, 4143–4150. [CrossRef]
9. Emmanuel, R.; Johansson, E. Influence of urban morphology and sea breeze on hot humid microclimate: The case of Colombo, Sri Lanka. *Clim. Res.* **2006**, *30*, 189–200. [CrossRef]
10. Chatzidimitriou, A.; Yannas, S. Street canyon design and improvement potential for urban open spaces; the influence of canyon aspect ratio and orientation on microclimate and outdoor comfort. *Sustain. Cities Soc.* **2017**, *33*, 85–101. [CrossRef]
11. Karimimoshaver, M.; Khalvandi, R.; Khalvandi, M. The effect of urban morphology on heat accumulation in urban street canyons and mitigation approach. *Sustain. Cities Soc.* **2021**, *73*, 103127. [CrossRef]
12. Huo, H.; Chen, F.; Geng, X.; Tao, J.; Liu, Z.; Zhang, W.; Leng, P. Simulation of the urban space thermal environment based on computational fluid dynamics: A comprehensive review. *Sensors* **2021**, *21*, 6898. [CrossRef] [PubMed]
13. Hu, G.; Liu, L.; Tao, D.; Song, J.; Tse, K.T.; Kwok, K.C. Deep learning-based investigation of wind pressures on tall building under interference effects. *J. Wind Eng. Ind. Aerodyn.* **2020**, *201*, 104138. [CrossRef]
14. Hepburn, C.; Qi, Y.; Stern, N.; Ward, B.; Xie, C.; Zenghelis, D. Towards carbon neutrality and China's 14th Five-Year Plan: Clean energy transition, sustainable urban development, and investment priorities. *Environ. Sci. Ecotechnol.* **2021**, *8*, 100130. [CrossRef] [PubMed]
15. Atwal, K.S.; Anderson, T.; Pfoser, D.; Züfle, A. Predicting building types using OpenStreetMap. *Sci. Rep.* **2022**, *12*, 19976. [CrossRef]
16. Gong, X.; Li, Y.; Cai, J.; Ma, Z.; He, S.; Pan, B.; Lei, X. A Statistical Analysis of Energy Consumption Survey of Public Buildings in a Hot Summer and Cold Winter Coastal Zone of China. *Buildings* **2023**, *13*, 2685. [CrossRef]
17. Hong, Y.; Ezeh, C.I.; Deng, W.; Hong, S.-H.; Peng, Z. Building energy retrofit measures in hot-summer–cold-winter climates: A case study in Shanghai. *Energies* **2019**, *12*, 3393. [CrossRef]
18. Guo, F.; Schlink, U.; Wu, W.; Mohamdeen, A. Differences in Urban Morphology between 77 Cities in China and Europe. *Remote Sens.* **2022**, *14*, 5462. [CrossRef]
19. Sobrino, J.A.; Jiménez-Muñoz, J.C.; Paolini, L. Land surface temperature retrieval from LANDSAT TM 5. *Remote Sens. Environ.* **2004**, *90*, 434–440. [CrossRef]
20. Zhang, M.; Gao, Z. Effect of urban form on microclimate and energy loads: Case study of generic residential district prototypes in Nanjing, China. *Sustain. Cities Soc.* **2021**, *70*, 102930. [CrossRef]
21. Zhu, S.; Chen, M.; Lu, S.; Mai, X. Influence of Urban Geometry on Thermal Environment of Urban Street Canyons in Hong Kong. *Buildings* **2022**, *12*, 1836. [CrossRef]
22. Hössjer, O. On the coefficient of determination for mixed regression models. *J. Stat. Plan. Inference* **2008**, *138*, 3022–3038. [CrossRef]
23. Yang, X.; Zhao, L.; Bruse, M.; Meng, Q. Evaluation of a microclimate model for predicting the thermal behavior of different ground surfaces. *Build. Environ.* **2013**, *60*, 93–104. [CrossRef]
24. Willmott, C.J. Some comments on the evaluation of model performance. *Bull. Am. Meteorol. Soc.* **1982**, *63*, 1309–1313. [CrossRef]
25. Narimani, N.; Karimi, A.; Brown, R.D. Effects of street orientation and tree species thermal comfort within urban canyons in a hot, dry climate. *Ecol. Inform.* **2022**, *69*, 101671. [CrossRef]
26. Alsaad, H.; Hartmann, M.; Hilbel, R.; Voelker, C. The potential of facade greening in mitigating the effects of heatwaves in Central European cities. *Build. Environ.* **2022**, *216*, 109021. [CrossRef]
27. Battista, G.; Carnielo, E.; Vollaro, R.D.L. Thermal impact of a redeveloped area on localized urban microclimate: A case study in Rome. *Energy Build.* **2016**, *133*, 446–454. [CrossRef]
28. Li, J.; Zheng, B. Does Vertical Greening Really Play Such a Big Role in an Indoor Thermal Environment? *Forests* **2022**, *13*, 358. [CrossRef]
29. Aboelata, A. Vegetation in different street orientations of aspect ratio (H/W 1: 1) to mitigate UHI and reduce buildings' energy in arid climate. *Build. Environ.* **2020**, *172*, 106712. [CrossRef]
30. Tan, X.; Liao, J.; Bedra, K.B.; Li, J. Evaluating the 3D cooling performances of different vegetation combinations in the urban area. *J. Asian Archit. Build. Eng.* **2022**, *21*, 1124–1136. [CrossRef]
31. Ziaeemehr, B.; Jandaghian, Z.; Ge, H.; Lacasse, M.; Moore, T. Increasing solar reflectivity of building envelope materials to mitigate urban heat islands: State-of-the-art review. *Buildings* **2023**, *13*, 2868. [CrossRef]
32. Rajan, E.H.S.; Amirtham, L.R. Urban heat island intensity and evaluation of outdoor thermal comfort in Chennai, India. *Environ. Dev. Sustain.* **2021**, *23*, 16304–16324. [CrossRef]
33. Jamei, E.; Rajagopalan, P. Effect of street design on pedestrian thermal comfort. *Archit. Sci. Rev.* **2019**, *62*, 92–111. [CrossRef]
34. Lin, Y.; Ichinose, T.; Yamao, Y.; Mouri, H. Wind velocity and temperature fields under different surface heating conditions in a street canyon in wind tunnel experiments. *Build. Environ.* **2020**, *168*, 106500. [CrossRef]
35. Kang, E.; Lee, R.; Yoon, J.; Cho, H.; Kim, D. Uncertainty Assessment of Mean Radiant Temperature Estimation for Indoor Thermal Comfort Based on Clustering Analysis of Reduced-Input Surfaces. *Buildings* **2023**, *13*, 342. [CrossRef]

36. Peeters, A.; Shashua-Bar, L.; Meir, S.; Shmulevich, R.R.; Caspi, Y.; Weyl, M.; Motzafi-Haller, W.; Angel, N. A decision support tool for calculating effective shading in urban streets. *Urban Clim.* **2020**, *34*, 100672. [CrossRef]